IEEE Access
Multidisciplinary | Rapid Review | Open Access Journal

Received June 14, 2020, accepted June 22, 2020, date of publication July 1, 2020, date of current version July 21, 2020.

Digital Object Identifier 10.1109/ACCESS.2020.3006346

Security Assured CNN-Based Model for Reconstruction of Medical Images on the Internet of Healthcare Things

SUJEET MORE[1], JIMMY SINGLA[1], SAHIL VERMA[1], (Member, IEEE), KAVITA[1], (Member, IEEE), UTTAM GHOSH[2], (Senior Member, IEEE), JOEL J. P. C. RODRIGUES[3,4], (Fellow, IEEE), A. S. M. SANWAR HOSEN[5], AND IN-HO RA[6], (Member, IEEE)

[1]School of Computer Science and Engineering, Lovely Professional University, Phagwara 144411, India
[2]Department of EECS, Vanderbilt University, Nashville, TN 37235, USA
[3]Electrical Engineering, Federal University of Piauí (UFPI), Teresina 64049-550, Brazil
[4]Covilhã Delegation, Instituto de Telecomunicações, 3030-290 Coimbra, Portugal
[5]Division of Computer Science and Engineering, Jeonbuk National University, Jeonju 54896, South Korea
[6]School of Computer, Information and Communication Engineering, Kunsan National University, Gunsan 54150, South Korea

Corresponding author: In-Ho Ra (ihra@kunsan.ac.kr)

This work was supported in part by the Human Resources Development Program of the Korea Institute of Energy Technology Evaluation and Planning (KETEP) under Grant 20194010201800, in part by the Korean Government and Institute for Information and Communications Technology Promotion (IITP) Grant funded by the Korean Government (MSIT) under Grant 2018-0-00508, in part by the Development of Blockchain-Based Embedded Devices and Platform for MG Security and Operational Efficiency, in part by the FCT/MCTES through national funds and when applicable co-funded EU funds through the Project under Grant UIDB/EEA/50008/2020, and in part by the Brazilian National Council for Research and Development (CNPq) under Grant 309335/2017-5.

ABSTRACT Medical Imaging is the most significant technique that constitutes information needed to diagnose and make the right decisions for treatment. These images suffer from inadequate contrast and noise that occurs during image acquisition. Thus, denoising and contrast enhancement is crucial in increasing the visual quality of the images for obtaining quantitative measures. In this research, an innovative and improvised denoising technique is implemented that applies a sparse aware with convolution neural network (SA_CNN) for investigating various medical modalities. To evaluate and validate, the convolution neural network utilizes patch creation and dictionary methods for obtaining information. The proposed framework is predominant to other current approaches by employing image assessment quantitative measures like peak signal to noise ratio (PSNR), structural similarity index (SSIM), and mean squared error (MSE). The study also optimizes the computational time to achieve increased efficiency and better visual quality of the image. Furthermore, the widespread use of the Internet of Healthcare Things (IoHT) helps to provide security with vault and challenge schemes between IoT devices and servers.

INDEX TERMS Convolution neural network, denoising, security, internet of healthcare things (IoHT), peak signal to noise ratio, restoration, structural similarity index.

I. INTRODUCTION

The Internet of Things (IoT) is a heterogeneous network of physical objects (things) that are embedded with electronics, RFID tags, sensors, software, and actuators to connect and exchange a large volume of data with other devices over the Internet and offer any service, at any time, anywhere and any network. It makes the physical infrastructures smarter, secure, and reliable, and fully automated systems. These physical infrastructures include buildings (homes, schools, offices, factories, etc.), utility networks (power grid, gas, water, etc.), transportation networks (roads, railways, airports, harbors, etc.), vehicles (cars, rails, planes, etc.), waste management, security and emergency systems, industrial control, and healthcare systems [1], [2]. On the Internet of Healthcare Things (IoHT), the sensor-based devices are incorporated with IoT and integrated with mobile technologies to collect the data and combine with electronic health record (EHR) systems for providing seamless connectivity with efficient utilization of resources in healthcare systems.

The associate editor coordinating the review of this manuscript and approving it for publication was Gautam Srivastava.

It has the potential to give rise to many medical applications such as remote patient monitoring, chronic diseases, elderly care, treatment progress, observation, and consultation. IoHT uses sensor-based devices to track biological conditions or symptoms of patients, such as euthermia, blood pressure, heart rate, blood glucose, brain activities, gesture, or contaminants, and to collaboratively transmit their sensed data through a communication media to primary healthcare service. The healthcare services provided by IoHT are expected to reduce the costs, increase the quality of life, and enrich the experience of users.

Images ideally are the most powerful tool of information widely used in all outperforming areas. Image processing is considered one of the diverse and complex fields with the growth of advanced systems, which facilitates us to refine these images to improve their quality. Many medical modalities like X-ray, Computed Tomography (CT) Scan, Positron Emission Tomography (PET), Ultrasound, and Magnetic Resonance Imaging (MRI) achieved a breakthrough in diagnosing diverse diseases. These modalities suffer from problems that may cause an inaccurate prediction during diagnosis. Among all these modalities magnetic resonance images are powerful for providing detailed information of the internal body. These magnetic resonance images also suffer from some limitation of acquisition time and spatial resolution, which degrades the superiority of the image by introducing noise at the time of processing. The acquisition process of magnetic resonance images gets overwhelmed by diverse kinds of noises. Sonali *et al.* [3] discuss a variety of noise, such as Gaussian noise or type 1, uniform noise or type 2, impulse noise or type 3, speckle noise, and positron variance noise, etc. The type 1 noise is caused by natural radiations and vibrations. Impulse noise drops the values or pixels of the initial image [4]. The noise-induced by environmental circumstances is speckle noise. These induced noise or artifacts reduce and affect the precision and efficiency of the automated system for disease diagnosis [5]. These noisy data and unclear image lead to unsatisfactory results and is a serious issue to patients' treatment. Also, the well-contrasted image leads to an improved interpretation of soft and hard tissues providing sufficient computation for segmentation, feature extraction, and classification of these tissues.

Generally, the ultrasound images and magnetic resonance images are deployed on low thickness tissues or soft tissues such as ligaments and cartilages. The X-ray is employed on high-density tissues or hard tissues like bones. Restrictive factors such as intrinsic features and high cost of the imaging system, due to which images always prone to inadequate contrast and noise issues. So denoising and enhancement become an essential and informative means to increase the quality of the image for efficient and precise outcomes in real-world applications. The X-ray is low contrast with the reduced ability and few details within the image due to high penetration, radiations, and blurring. The images containing the soft tissues and bone structure get affected due to radiations and blurring effects due to the patient's moment. The X-ray images also endure from artifacts due to variations in photon intensity and digitizing the images.

The computer tomography images have a high contrast narrow range grayscale features for detailed classification of tissues. These CT images provide an imbalanced foreground of vessels, organs, etc. These images suffer from inaccurate edges between vessels and organs. The magnetic resonance images offer more detailed information about soft tissues and provide more acute detection. The magnetic resonance images are made due to the effect of fluid [32] and variations at the periphery area of the hemispheres and around the cerebrospinal fluid. These magnetic resonance images suffer from poor contrast (visual quality) and readability for the treatment of diseases. Low-quality representation of detailed information of an image while capturing with numerous devices or tools may cause an imprecise treatment of disease diagnosis. Generally, the images are captured by electronic magnetic signals into humans and reminisce about the reflexes. These EM signals are injurious to the tissues and not preferred for capturing the multiple medical images. The images are of irregular contrast, some with (too dark and too bright). The images like X-ray and magnetic resonance imaging have a larger background scene that induces the artifacts in the medical image.

The motivation for this study is as follows; (i) the low quality of medical modality provides inaccurate information and diagnosis. (ii) Sensitive patients' health records in public networks are a prime target for attackers. The images are prone to noise, artifacts, and low quality; due to electromagnetic signals, and irregular brightness obtained during the acquisition process. To resolve the problem of noise and low quality, in this research work, a novel innovative framework is proposed for denoising and contrast enhancement with preserving the details like edges and texture of the images. The sparse aware CNN is used for optimization with some fine parameters. The foremost involvement of the framework is to improvise the contrast quality and eliminate noise for all types of medical images. The efficiency of the framework is measured using peak signal to noise ratio and structural similarity index. To overcome the problems, an efficient and effective technique is required to handle the large volume of the dataset. In the recent past, the Convolution neural network (CNN) has gained a lot of attention to overcome the issue of large volume datasets due to its robustness and easy training of the data. CNN can reduce the noise and increases the visual contrast in the magnetic resonance images and reconstructs the image by preserving the details or edges. Therefore, the special properties of CNN make different from other existing state-of-the-art techniques mentioned in literature. This research helps to resolve the speed and high-quality issues related to medical images with high efficiency.

Contribution of the study aimed at the following concepts; (i) to solve issues related to high-quality image reconstruction, (ii) computational speed issues for bulky image sets, and (iii) securely communicate medical images between IoT devices and server. The proposed research work presented

a state-of-the-art generalized hybrid convolution neural network algorithm (SA_CNN) for reconstructing the high visual quality magnetic resonance image. The novel Sparse Aware CNN model eliminates various noises such as Gaussian noise, Rician noise, and Speckle noise. Along with the CNN model, a dictionary learning algorithm is integrated to increase the training speed of the dataset. This dictionary learning approach makes the model more reliable and computationally efficient. The proposed framework divides the image into numerous patches and provides these to the pipelined architecture (CNN) then the difference weight is stored in the dictionary for training data. Then, this generated dictionary is utilized for the testing phase to reconstruct the high visual quality and denoised image. Further, the denoised images were transferred to the cloud-assisted IoT for providing access to concerned stakeholders via a gateway. The proposed framework achieves a high outcome with performance measures.

The organization of the research work is as follows: the literature review, methodology, and proposed approach are discussed in section 2 and section 3 respectively. Section 4 and section 5 describes experimentation and illustrates the outcomes of the proposed research work. The discussion and conclusion of the work are presented in section 6.

II. RELATED WORK

In the recent past, numerous investigations have dealt to eliminate or reduce the noise and improve the visual contrast of magnetic resonance images. These medical images suffer from a lot of problems, so they require enhancement and reconstruction. One of the studies done by C. Rubina and Ravichandran *et al.*, in [6], [7] where the images were filtered using adaptive histogram equalization and compared with the CLAHE method. The mean and median filters were applied for estimating the probability of each occurrence of each pixel. To overcome the cons of the histogram equalization method, a new technique was introduced Bi-histogram equalization which splits the original image into 2 sub-divisions founded on the average value of brightness of all the pixels. The dynamic histogram equalization divides the histogram-based image without the mean and median values but causes saturation and insufficient smoothening. The amount of intensity provides the contrast enhancement for an image. The contrast limited adaptive HE introduced by Nema Salem *et al.*, in [8], divides the image into several equal-size regions. Then the clipping region was estimated and cumulative distribution is calculated with adjoining grid points. The contrast limited adaptive HE performs best for few images like retina while it degrades its performance for knee, brain magnetic resonance images. The contrast levels of the image can be increased with the ABC algorithm developed by Jai Chen *et al.*, which is given in [9]. This ABC method generates the optimal solution with the 2-fold approach. Initially, the quality of the image was calculated, then a new pixel intensity is estimated using transformation function. The ABC method provides efficient and faster processing than traditional approaches, to accomplish well outcomes given PSNR and SSIM.

Contrast stretching is to stretch all the intensities of the image, using the discrete wavelet transform technique in [10] was proposed by Aqilah. H *et al.* The wavelet transforms method uses the scaling function to approximate an image function at different levels. This method achieves a better result in regards to signal to noise ratio and standard value. The adaptive histogram equalization with intensity replacement utilized by ISA *et al.* was introduced in [11]. This method was applied to Flair images with adjustment in intensity and contrast mapping. The method enhances the contrast with region mapping on T2-weighted image hyper-intensities with estimating PSNR and gradient parameters. Improvised optimal contrast and edge enrichment method presented by Pankaj *et al.*, for images using Krill herd technique was introduced in [12]. Using the least and extreme average and intermediate histogram values, the KH method automatically adjusts the parameter with the fitness function. The method is only applicable to low-level grey images to enhance the fine details and diagnosis of disease.

The type 2 noise from magnetic resonance images reduces the accuracy of prediction, so an optimal algorithm implemented by Kaixin *et al.*, was introduced in [13]. This Non-local means method was enhanced and along with fuzzy c-means introduced a new method FANLM, which adjusts the window automatically instead of fixed size so to achieve a better result. If pixels are non-smooth then the size of the window will be big and the denoising region will be a blur and if the pixels are smooth then the window will be small and the resultant image will be different from the original image. The wavelet method was used for denoising the MRI in [14] with an estimation of PSNR and MSE. This method was developed by Md. Nabih Ali divides an image into a set of functions also known as wavelets. The experiment was conducted on 10dB wavelets with decomposition, and estimating the PSNR and MSE values and eliminating the Gaussian or type 1 and impulse noise. The deep learning model and the neural network model introduced by Xuexiao *et al.* were applied to various noises in [15]. The deep learning model accepts a small sample size and applied to eliminate only type 2 noise and the neural network model was applied to eliminate various noises with different levels. These 2 methods provided flexibility and various features of an image. These 2 models were applied in sub-intervals instead of applying as a whole interval to gain better performance.

The small sample size for the neural network in [16], the model was implemented using deep and wide CNN by Jianjun Yuan. Due to the flexibility and capacity to exploit the image characteristics of the deep learning method. The T1-weighted and T2-weighted brain MRI with different algorithms were compared where deep leaning performed better in terms of PSNR and SSIM. Fabio. B *et al.*, in [17] introduced a novel sparse tensor model based on the weighted regularization from MRI with efficient computation. The method

uses brain MR images for the study with 512 × 512 with 20 slices. The experiment was conducted on four different contrast models with PSNR and SSIM estimation. The sparse tensor model outperformed the better with the regularization of weighted pixels. Hemalata. V *et al.* used the KS method to denoising the images with Euclidean distance that was implemented in [18]. The Magnetic resonance images of the similar slices were obtained to exploit the statistical behavior using cumulative distribution function. The KS was applied for finding the similarity measure and computing the distance of the regularized pixel. The image comprises of many structural details which helps physician for diagnosing the diseases. The non-local means methods were discussed in [19] by M Elhonseny *et al.*, with their limitations and advantages. All the non-local means methods perform better in their context regarding the noise reduction with edge presentation.

To protect the data within the MRI such as structural surface or edges Matt Judson *et al.*, in [20] presented a method based on bilateral filter, which was utilized to categorize the denoised image as regular or irregular. The features such as error rate, peak signal to noise ratio are estimated using CNN classifier. A partial differential equation evaluated by J Mohan, based methods for denoising was presented in [21]. The computational efficiency of medical images is to be optimally applied to a larger size and block-wise computation using NLM methods enhances the performance of a new algorithm. Removing the type 2 noise from MR images [22] was presented by Hari Mohan *et al.*, using median and Weiner filters. The efficiency of the median filter is good given total variation minimizing scheme and diffusion filter. The NS Weiner filter tends to produce good results compared to other methods preserving the quality details of the image. The discrete wavelet transform used [23] is applied by M. Sahnoun *et al.*, to numerous categories of noise and diminishes the precision of the investigation system. The PSNR and noise density values of an image were estimated with a comparative analysis of three different methods. The method reduces the salt and pepper, type 1, and speckle noise with 0.1, 0.3, 0.5, and 0.7 variances. The discrete wavelet transform method was used for enhancing the quality of the image in [23]. The T1-weighted image of the brain was used in the wavelet transform method. The method estimates the grey matter, white matter, and cerebrospinal fluid also was calculated the PSNR, SSIM, and few parameters signifying the visual quality of the image.

The overhead approaches have noteworthy involvement in their specialized area of involvement but not either of them is an efficient and precise method for reducing noise and enhancing the contrast from MRI. The denoising and contrast enhancement of images should have superior PSNR and SSIM values to preserve the details within the image unaffected. Several, noise reduction and contrast enhancement techniques discussed above have either superior PSNR or superior SSIM, not both with greater value. In this research work, an innovative novel hybrid approach was introduced to denoise and progress the visual quality details of the medical images. This approach can be applied to any kind of images with different noise levels. This method provides high PSNR and SSIM values. Gai *et al.* [38] introduced a loss function with improved CNN (MP-DCNN) for the noisy image. SegNet is combined with this method for retaining edge information. Tian *et al.* [39] introduced batch renormalization (BRDNet) by combing two networks to increase the depth. It solves the problem of input data with small batches. Hamid *et al.* [40] introduce a deep CNN to preserve the edges in the image. The canny algorithm used with method provides smoothing noise for superior outcomes.

Yan *et al.* implemented the computational complexity of magnetic resonance image reconstruction with mobile computing-based IoT [36]. The reconstruction framework with compressed sensing was flexible on low-resolution images. Image fusion and interpolation were used to improve the quality of the MRI. The Internet of Healthcare Things (IoHT) suffers from privacy concerns. Yingnan *et al.*, [33] discuss a few security concerns on wireless systems. The updated antivirus patches and libraries provide a sufficient advantage to the system. The optimization approach on IoT introduced by Taha *et al.*, [34] uses domain knowledge with training data and relation extraction in feature space. Few concepts related to multimedia, spatial, moving things discussed by Khalid *et al.*, [35] helps to gain knowledge related to a diverse variety of IoT. A hybrid discrete model consisting of IoHT was introduced by Elhoseny *et al.*, [37] for medical data. The DWT resolves the issue of noise from the image in the IoT environment and evaluated the performance with PSNR, MSE, and SSIM parameters.

III. METHODOLOGY

The proposed model conferred for noise reduction and contrast enhancement of images in subsequent steps. First, the medical images are preferred from the dataset [28] and its replicant copy is attained by adding the image with three different kinds of noise, gaussian noise, impulse noise, and speckle noise [29]–[31]. The procedure of the proposed framework is discussed in the subsequent subsection.

The reason for CNN's success is its architecture that includes an initial parameter, gradient parameter, and rectified linear unit (ReLU). Although CNN achieves good outcomes, they suffer from gradient problems and makes difficulty in training networks. The performance of medical image processing in the field of CNN is very effective for feature extraction to denoise the images. In the proposed model dilated convolution as illustrated in the figure. 1, is used to overcome two problems (i) The size of the network also stated as filter size, which results in overfitting problems and increasing the computational cost, and (ii) Depth of the network which leads to exploding gradients. The dilated filter can be expressed with size $(2f + 1)(2f + 1)$ with a convolution kernel of $3 * 3$.

Figure. 1., illustrates the depth of our proposed model that is 17 layers. The model has three kinds of layers in this network; Convolution (Conv), ReLU, and dilated convolution.

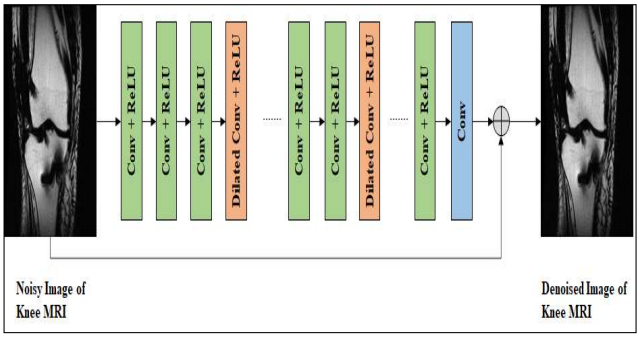

FIGURE 1. Proposed convolution neural network architecture.

The 1st and 16th layers are Conv + ReLU. The 2nd, 5th, 9th, and 12th layers are dilated convolution and the final layer is Conv. The size of the convolution kernel is $128 \times 1 \times 40 \times 40$ for the first and last layers. The size of other Conv kernel is $128 \times 64 \times 40 \times 40$.

A. NOISE MODEL REPRESENTATION

The noise of medical images is calculated using the magnitude of each pixel one by one. Since the noise cannot be represented using Gaussian distribution because of the nonlinearity of estimations, so the noise can be represented using probability distribution function with pixel intensity in equation 1. Equation 1, is the objective function to train the SA_CNN model.

$$P_m(M) = \frac{M}{\sigma^2}\left(\frac{A^2 + M^2}{2\sigma^2}\right) I_o\left(\frac{A * M}{\sigma^2}\right) \tag{1}$$

where A is representing the original pixel intensity and M pixel intensity.

I0 = Bessel function of zeroth order.

σ = Standard deviation of type 1 noise.

The noise distribution ranging between a 1 and 3 can be Rician or type 2 and value above 3 cannot be type 2 but tends towards Gaussian distribution or type 1. The Rician value equal to zero is also known to be as Rayleigh distribution or type 3 where no noise is present in magnetic resonance images.

$$\begin{aligned} \frac{A}{\sigma} &= 0 Rayleigh \\ 1 \leq \frac{A}{\sigma} &\leq 3 Rician \\ \frac{A}{\sigma} &\geq 3 Gaussian \end{aligned} \tag{2}$$

B. DISTRIBUTION OF NOISE

Generally, it is presumed that the image is damaged with the noise of type 1, which is quite simple and easy to deal with, and the signal reliant on and development model deviations it to type 2. The type 2 noise reduces the visual quality details of the image quantitatively and qualitatively. Type 2 assumption is given by equation 3

$$Y = Y_{re} + jY_m \tag{3}$$

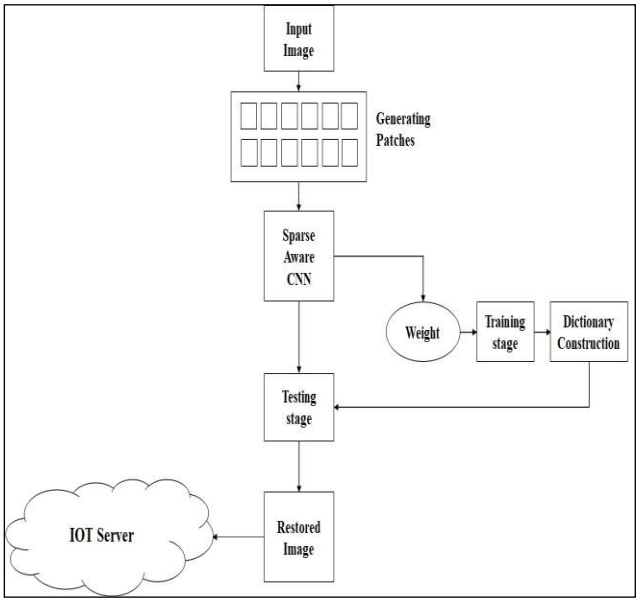

FIGURE 2. Proposed sparse aware convolution Neural Network (SA_CNN) architecture with patch creation.

where Yre and Ym are actual and unreal values in the image. These values are pretentious by ξ_1 and ξ_2, where ξ_1 and ξ_2 are the noise of type 1 with nil average and standard deviation σ.

$$Y_{re} = I\cos\theta + \xi_1 \tag{4}$$

$$Y_m = I\sin\theta + \xi_2 \tag{5}$$

here I, the original image and $\ominus$ is the segment value. An irregular noisy image is signified as a degree of the raw $Y = Y_{re} + jY_m$ image, represented by equation 6.

$$|Y| = \sqrt{(I\cos\theta + \xi_1)^2 + (I\sin\theta + \xi_2)^2} \tag{6}$$

The estimation of type 2 noise is squared of the magnitude of the bias in the image.

$$|Y|^2 = \sqrt{(I\cos\theta + \xi_1)^2 + (I\sin\theta + \xi_2)^2} \tag{7}$$

The noise is estimated by contextual areas [24]. The estimation of type 2 noise in the image is calculated by the statistical approach like MLE signal construction [25]–[27].

C. SA_CNN FRAMEWORK

The flow chart for the proposed framework is shown in Figure. 2, and discussed in detail:

Step 1: The initial step, the least visual contrast, and the irregular noisy image are preferred.

Step 2: Divide the image into patches randomly.

Step 3: Apply Sparse aware CNN to training dataset with generating weights.

Step 4: Create a dictionary with collecting values from the training stage.

Step 5: Test the dataset for noise elimination with dictionary knowledge.

Step 6: The restoration of the image is done for the quality of the image.

TABLE 1. Distribution of training data.

Ultrasound	CT Scan	T1-weighted	T2-weighted	FLAIR
50	15	630	355	150

Step 7: Store the denoised images to IoT (cloud-assisted) server.

1) TRAINING PHASE

Training is an important stage to efficiently increase the performance of the system. But normally the training phase takes long training time and complex process to train the image data. So, there is a need for designing an efficient technique to train the system faster and with less computational time. The proposed novel sparse aware convolution neural network is an effective technique to eliminate noise and to enhance the contrast. The model is trained on greyscale images of different types with sparse aware CNN generating weights for each layer. Then the dictionary is created which helps achieve the high-quality denoised image. We choose 1,200 images with size 512 × 512 for training the model. Table 1 describes the distribution of training data.

2) DICTIONARY

Due to the diverse variety of Convolution neural network features, the model adopted a specific dictionary D = [d1, d2…dn] have labels for each subject. Dictionary is represented using an equation 8, where noise is represented with k which is merged with input image patch i,

$$Y = i + k \tag{8}$$

The size of each patch is set as m X m where k lies between 8 and 12 values. The patches which are overlapped can be measured by the averaging process. The additive white type 1 noisy error can be eliminated by a predefined function provided by pseudo normalization estimated by equation 9.

$$\min ||\alpha||_0 \;\; s.t \;\; ||D_\alpha - Y||_2 \leq \in \tag{9}$$

The factor $\in$ can be chosen in such a way that approximation norm error $||\mathbb{D}_\alpha - \mathbb{Y}||_2$ can be defined by its variance. The quality of the image is achieved by using a sliding window concept. The dictionary scheme reduces the optimization problem by utilizing 15% of training time while denoising the images. This dictionary scheme does not require any heuristic knowledge and can adapt to the environment. The algorithm 1 demonstrates the dictionary creation technique. The dictionary is divided into rows and columns with an objective function $\mathrm{dj} = \mathrm{X}\,\mathrm{Z}_\mathrm{j}^\mathrm{T}/\|X\mathrm{z}_\mathrm{j}^\mathrm{T}\|2$ The dictionary updating is as follows; Let Z denotes weighted sparse coefficient and $\mathrm{D_i}$ be a dictionary

$$D_i = \min ||X - D_i Z||_f^2, ||_2 \leq 1 \tag{10}$$

3) TESTING PHASE

The testing phase is more efficient and flexible due to pre-trained data and patch-wise classification. A similar dictionary is provided in the testing phase by equation 11.

$$i^{\wedge} = i^{-} + \frac{(F(Y-Y)^2 - \sigma^2)(Y-i)}{F(Y-Y)^2} \tag{11}$$

where $\boldsymbol{\sigma}$ defines the noise level. The computation $\bar{\boldsymbol{i}}$ can is effectively utilized by a window size of m X k with a probability distribution function represented in equation 12.

$$i^{(t+1)} = i^t + n[\sum_{r=1}^{k} N_r * \psi_r(N_r * i^t) + [\frac{\lambda}{\sigma^2}(Y - i^t)]] \tag{12}$$

where $\mathbf{N}_r^-$ shows central pixel and convolution are defined by $*$ sign and $\boldsymbol{\eta}$ used to evaluate step size. To maintain the trade-off between likelihood and priori $\boldsymbol{\lambda}$ is utilized. The final value of $\boldsymbol{\lambda}$ relies upon noise level $\boldsymbol{\sigma}$. Once the dictionary has been trained, it could be utilized for classification job. According to the diverse scheme, the dictionary can be used for diverse classification jobs.

Algorithm 1 Creation of Dictionary for Preprocessing Step

Input

A training subset from class i, the coefficients Zi, the dictionary Di

Let Zi = [z1, z2, ……, zn] and Di = [d1, d2, …, dn] where i = 1,2, …, n, ith is the row vector of Zi and jth is the column vector of Di

for j = 1 **to** n **do**

Fix all di, 1 ≠ j, and update dj. Let X be the minimization function

Min $\mathrm{d_j} = \|\mathrm{X} - \mathrm{d_i Z_j}\|\mathrm{s.t.}\|\mathrm{d_j}\|2 - 1$

By solving this objective function

$\mathrm{dj} = \mathrm{X}\,\mathrm{Z_j^T}/\|\mathrm{Xz_j^T}\|2$

end for

Output

Update the Di (equation 10)

D. INTERNET OF HEALTHCARE THINGS (IoHT)

The Internet of Things (IoT) cloud is increasingly becoming more requested in the healthcare context for testing and clinical trials. The rapid development of IoT cloud has meant with healthcare systems (IoHT), that received less attention for medical image storage. The intelligent agents in the IoHT cloud provide proper decision support for proposed work by providing proper storage facilities [44]. The IoHT provides easy access to patients' information, remote medical consultations, and increased availability of medical data in real-time. It also provides high availability and scalability of data to both doctors and patients'.

Figure 3 illustrates the IoHT architecture to collect medical images in a secured and private IoT cloud. The patients connect to gateway through some terminal such as; computers or embedded devices. The user-terminal connects to the gateway through short coverage and low energy communication protocols such as; (IEEE 802.15.4 standard, 6LoWPAN, or Bluetooth). This gateway connects to a (medical) server or private cloud server for data storage and processing. On the

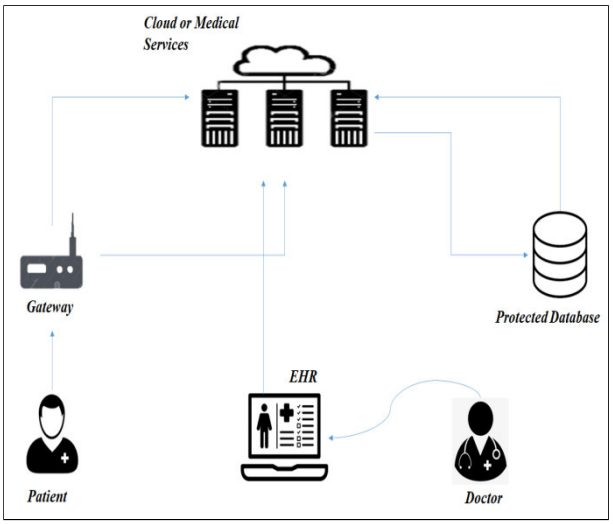

FIGURE 3. IoHT architecture for medical data storage.

other hand, patients' health records can be stored in electronic health records (EHR) and when the patient visits a doctor, she/he can access the records easily. The web-based module that allows data authorization and authentication for remote healthcare monitoring can be provided by some applications that include a user interface. The IoHT can provide support to elderly patients', suffering from chronic diseases. This aims to transmit, and securely store the medical images with addressing issues like interoperability between devices. Doctors may analyze medical images of the patients in remote locations and provide emergency assistance whenever necessary. IoHT provides support and concern in these categories; (i) remote monitoring (ii) healthcare assistance on smartphones (iii) security and privacy of medical images, and (iv) reducing time and increasing the quality of healthcare.

1) SECURITY MECHANISM WITH VAULT

The typical IoT architecture consists of three major components; (i) IoT device (ii) IoT (cloud-assisted) server, and (iii) communication gateway. The medical server (cloud-assisted IoT server) that communicates with clients uses single key authentication that is not sufficient for IoT devices to communicate with the server. There are few attacks such as, man-in-the-middle attack, DoS attack, and side-channel attack; that repossess the key shared during communication. Thus, a key change mechanism is the best solution to overcome this situation. In the model, we utilize a bunch of keys known as a safe vault. This secure vault, shares keys between both server and IoT devices. A typical 3-way validation between IoT device and server is utilized in the model. The device initiates the communication by conveying a request to the server, in response to that, the server sends a challenge to the IoT device. Then the device replies to the server with an authentication challenge. The server verifies the reply from the device if it is valid.

During this communication, both IoT devices and servers establish a shared key known as, session key. This session key is used for encrypting the messages between the device and

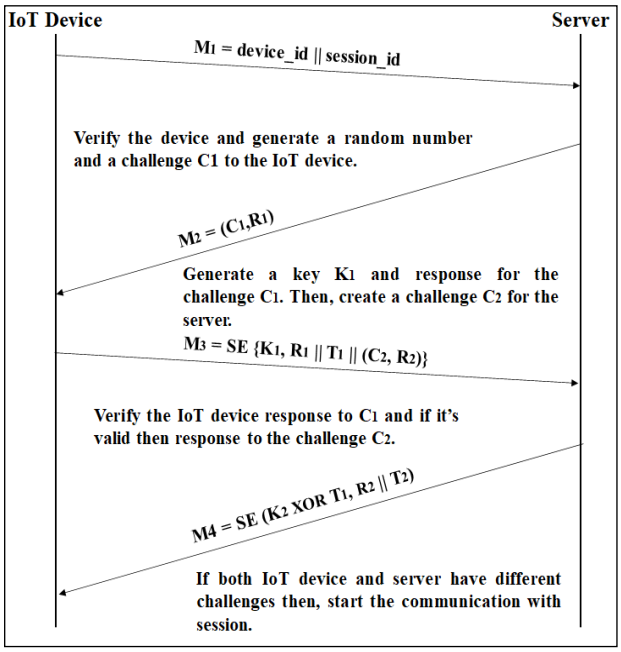

FIGURE 4. 3-Way message authentication.

the server. The secure and safe vault encompasses 'n' keys where each key is 'm' bits long, where 'm' represents the key size, and K[0], K[1], K[2],…., K[n−1] represents all keys. This secure vault is stored in a protected database.

2) CHALLENGE AND RESPONSE SCHEME

Our model uses a 3-way authentication scheme for mutual communication. Figure 4, illustrates the messages exchanged between the IoT device and server. This IoT device starts the communication by sending message M_1 to the server. This message contains session_id to keep the session alive. Then the server validates session_id and if the message is valid then, the server replies with challenging message M_2 to the device. This challenging message consists of a random number and challenge, R_1 and C_1 respectively. C_1 is a set of 'X' discrete values where every value denotes the index of a key. C_1 is represented as (C_{11}, C_{22}, ….., C_{1X}) where 'X' is less than n and M_2 are (C_1, R_1).

An impermanent key 'K_1' is generated of length' bits that perform XOR operation on every key of the same indices in C_1. So, K_1 is ($K[C_{11}] \oplus K[C_{12}] \oplus \ldots.. \oplus K[C_{1X}]$). Then the device responds to the challenge with shared key encryption on $R_1 || T_1$ with K_1 as an encryption key, where T_1 is a random number generated by the device. The device also initiates a challenge C_2 to the server with a set of 'X' random numbers (R_2) ranging between 0 to n−1. Both C_1 and C_2 should be different, if both are the same then the attacker can access the data during the C_2 challenge.

The server receives messages from IoT devices with the following sequence; $M_3 = SE\ \{K_1, R_1 || T_1\ (C_2, R_2)\}$, where SE represents shared key encryption. $K_1 = X[C_{11}] \oplus X[C_{12}] \oplus \ldots. \oplus X[C_{1X}]$ represents encryption key. Then, $C_2 = (C_{21}, C_{22}, \ldots., C_{2X})$ with R_2 random number for

the second challenge and T_1 random numbers for session key generation.

Message to IoT device from the server with following sequence; $M_4 = SE\ (K_2 \oplus T_1, R_2 || T_2)$, where, $K_2 = X[C_{21}] \oplus X[C_{22}] \oplus \ldots \oplus X[C_{2X}]$ and $K_2 \oplus T_1$ is the key for encryption with T_2 random numbers for session. The IoT device validates the uniqueness of the server by verifying the R2 value by decrypting the message M4 with $K_2 \oplus T_1$. After both IoT devices, and the server authenticates one another then, further communication for that session takes place with $T = T_1 \oplus T_2$, session key.

After every session, the secure vault's value changes based on the HMAC generation, which is a key-based hashing technique. The HMAC method works on the contents of the vault in the following manner; (i) HMAC of the key and existing vault is exchanged amongst the server and IoT device. The HMAC is represented with h = HMAC (existing vault, data exchanged). The existing value of vault is partitioned into 'j' equal parts of 'k' bits. Then, we perform (h ⊕ i), where 'i' is an index of vault partition. Zero (0) value, is padded to the end to create 'j' partitions if the vault is not divisible by 'k' bits.

To validate this model in our framework, we tested a hijack attack. This attack captures the communicated messages amongst the server and IoT device, by spoofing. The attacker can recognize itself as, a server to the IoT devices, and vice versa. In our model, a session key 'T' is generated to authenticate all communication between the device and server. The key to this session of communication is shared secretly with IoT devices and servers. So, a hijack attack is not possible to retrieve the messaged exchanged between IoT devices and server during communication.

IV. PERFORMANCE METRICS AND EXPERIMENT

In this study, a SA_CNN method is proposed with its depth the same as denoising CNN (DnCNN). The initial parameters are; (i) learning rate, alpha_1, alpha_2 and epsilon are $1*10^{-3}$, 0.9, 0.999 and $1*10^{-8}$ respectively. (ii) The number of batches is set to 226, and (iii) The number of epochs is 180 and the initial weights set to as shown in [38]. The learning rate of the epochs is $1*10^{-3}$ to $1*10^{-8}$.

We choose Anaconda 3 to train and test the model with all experiments implemented in the environment of Windows 10, run on 12 GB RAM, Intel i3- 7130U CPU with 2.70 GHz. The proposed denoising and contrast enhancement techniques are applied on a large number of datasets with quantitative analysis conducted on different efficiency parameters like peak signal to noise ratio (PSNR) and structural similarity index (SSIM). The proposed goal is examined with existing techniques like block-matching 3-D filter (BM3D), trainable nonlinear reaction difference (TNRD), denoising convolution neural network (DnCNN), improvised convolution neural network with loss function (MP-DCNN).

A. MEDICAL DATASET

The efficiency of the proposed framework is validated on a diverse dataset obtained from a reference source [28]. Table 2 demonstrates the dataset along with the source of the data. The dataset consists of 2,260 images of Ultrasound, CT Scan, and Magnetic Resonance Imaging used for training and testing. The images collected of Ultrasound are of resolution 390 × 330 pixels, CT scan images, T1-weighted magnetic resonance images of 512 × 512 pixels, T2-weighted images 512 × 512 pixels and Flair magnetic resonance images of 512 × 512 pixels. These medical images are collected from local hospitals whose patients' details are not disclosed.

TABLE 2. Different types of image dataset used in experimentation.

Sr No	Image Type	Number of Images	Description	Source
1	Ultrasound	80	Resolution 390 X 330 pixels (approx.)	Data collected from laboratory
2	CT Scan	20	Uncompressed 512 pixels	Data collected from laboratory
3	T1-weighted (T1-W) Knee MRI	960 images of 40 subjects	TE: 9.7 TR: 760.0	Local Hospital
4	T2-weighted (T2-W) Knee MRI	840 images of 35 subjects	TE: 34.7 TR: 2740.0	Local Hospital
5	Flair MRI	360 images of 15 subjects	TE: 104.9 TR: 3360.0	Local Hospital

B. PERFORMANCE MEASURES

The quantitative or measurable efficiency of the proposed denoising and contrast enhancement technique is estimated using the parameters like peak signal to noise ratio (PSNR) and structural similarity (SSIM) index. SSIM measures the superiority of margin between 2 image similarity in parameters of average intensity ($\mu 1$ and $\mu 2$). The parameter C (x1, x2) is the contrast enhancement function which computes the superiority of the image in terms of standard deviation ($\sigma 1$ and $\sigma 2$). The parameter S (x1, x2) is a structural assessment function.

1) STRUCTURAL SIMILARITY (SSIM) INDEX

The SSIM is utilized for estimating the resemblance among two images. Generally, methods to estimate of the images like PSNR and MSE are enhanced by SSIM. SSIM provides the measure of image quality degradation with structural details. The SSIM is estimated on several windows of an image. Equation 13 and 14 represent the SSIM and simplified version of SSIM respectively.

$$SSIM(x_1, x_2) = [L(x_1, x_2)a_1]^*[C(x_1, x_2)b_1]^*[S(x_1, x_2)c_1] \tag{13}$$

$$SSIM(x_1, x_2) = \frac{(2\mu_1\mu_2 + U_1)(2\sigma_{12} + U_2)}{(\mu_1 + \mu_2 + U_1)(\sigma_1 + \sigma_2 + U_2)} \tag{14}$$

where, $\mu 1$ is an average of the first image, $\mu 2$ average od second image. $\sigma 1$ and $\sigma 2$ are the variances of the first and second images respectively. $\sigma 12$ represents the covariance of both images. U1 and U2 are two variables for stabilizing weak denominator.

2) PEAK SIGNAL TO NOISE RATIO (PSNR)

The PSNR is abbreviated as a peak signal to noise ratio and well-known to be a fraction among the extreme intensity of the signal and intensity of the irregular noise that alters the representation. The quality of the restoration of an image is evaluated by PSNR. The highest value of PSNR specifies the superior quality of the reconstructed image. The PSNR value is well-defined with mean squared error (MSE) which utilizes two p X q grayscale images. The Peak Signal to Noise Ratio (PSNR) is estimated using equation 15.

$$PSNR(dB) = \frac{10\log_{10}(L-1)^2}{MSE} \tag{15}$$

3) MEAN SQUARED ERROR (MSE)

The MSE is used to compare the compression quality of the original and compressed image with cumulative squared error. The lower the MSE, the lower the error value that is evaluated as shown in equation 16.

$$MSE = \frac{\sum_{M,N}[I_1(m,n) - I_2(m,n)]^2}{M^*N} \tag{16}$$

V. RESULTS AND DISCUSSIONS

This section demonstrates the outcome achieved using the proposed framework and comparison with different methods. The experimental outcomes are accomplished with T1-weighted, T2-weighted, Flair 1.5 T magnetic resonance images. Two quantitative measures such as PSNR, SSIM are utilized for demonstrating the comparative analysis of the novel proposed model with other relative techniques. At the beginning of the experiment, the images are preferred from the dataset and added with a noise like gaussian, salt-pepper, and speckle noise in the image. This tainted image with different noise is denoised using the proposed framework. The outcome of the proposed model is validated with real medical data to improve the performance. The histogram equalization (HE) is the most used technique in the literature review with many improvements. Contrast enhancement and denoising in histogram equalization are achieved using stretching and flattening of greyscale images. The proposed model uses the patch technique to divide the image into several small regions and then applies the sparse aware Convolution neural network.

Table. 3, illustrates the comparative analysis of different techniques with the proposed model with average PSNR and SSIM parameters. The PSNR and SSIM value obtained by the proposed framework compared with different methods is better. The PSNR value of 39.368 dB and SSIM value of 0.8561 which is highest among all. Table 4, tabulated the PSNR value for all types of images and compared with different methods. The PSNR value gained for different images is ranged from ∼23.11 dB to ∼46.81 dB.

TABLE 3. Average PSNR and SSIM value of different methods.

	TNRD [42]	BM3D [41]	DnCNN [43]	MP-DCNN [38]	SA_CNN
PSNR	23.89	27.62	29.87	28.44	39.368
SSIM	0.8184	0.8306	0.8330	0.8486	0.8561

TABLE 4. PSNR (dB) value for different modalities.

Modalities	TNRD [42]	BM3D [41]	DnCNN [43]	MP-DCNN [38]	SA_CNN
Ultrasound	24.23	25.66	25.83	27.49	29.13
CT Scan	25.54	26.81	29.36	28.64	35.59
T1-weighted MRI	23.11	28.63	30.56	29.23	41.72
T2-weighted MRI	23.43	29.18	32.47	28.84	43.81
FLAIR MRI	23.14	27.81	31.12	28.02	46.59

TABLE 5. SSIM value for different modalities.

Modalities	TNRD [42]	BM3D [41]	DnCNN [43]	MP-DCNN [38]	SA_CNN
Ultrasound	0.8004	0.8012	0.8123	0.8136	0.8225
CT Scan	0.8165	0.8231	0.8254	0.8303	0.8437
T1-weighted MRI	0.8145	0.8538	0.8164	0.8554	0.8509
T2-weighted MRI	0.8487	0.8460	0.8544	0.8711	0.8747
FLAIR MRI	0.8119	0.8291	0.8569	0.8727	0.8789

Table. 5, demonstrates the SSIM values for different types of images and it shows that the FLAIR image gained the highest value with 0.8789 and ∼0.85 for all other magnetic resonance images. MSE value is demonstrated in the table. 6, with an approximate value of 0.004 for the proposed method. Table. 7, illustrates the computation time for all the methods. The proposed framework will achieve a great computation time with 1.44s which is less compared to all other methods. These values demonstrate the sparse aware convolution neural network (SA_CNN) is best suited for noise elimination and increasing the visual quality of medical images.

The assessment of peak signal to noise ratio (PSNR): Estimates the proportion among the extreme value of the signal and the power of misrepresenting noise that disturbs the superiority. PSNR value of the proposed model is the highest among all other methods up to 46dB. The structural similarity index (SSIM) is a metric to estimate the resemblance between 2 images. Higher the value of SSIM,

TABLE 6. MSE value for different modalities.

Modalities	TNRD [42]	BM3D [41]	DnCNN [43]	MP-DCNN [38]	SA_CNN
Ultrasound	0.015	0.013	0.015	0.012	0.005
CT Scan	0.011	0.013	0.013	0.011	0.003
T1-weighted MRI	0.015	0.012	0.013	0.013	0.004
T2-weighted MRI	0.003	0.003	0.003	0.003	0.006
FLAIR MRI	0.012	0.012	0.012	0.012	0.005

TABLE 7. Execution time (seconds) for different methods.

Methods	TNRD [42]	BM3D [41]	DnCNN [43]	MP-DCNN [38]	SA_CNN
Execution Time	5.51	11.89	3.41	2.96	1.44

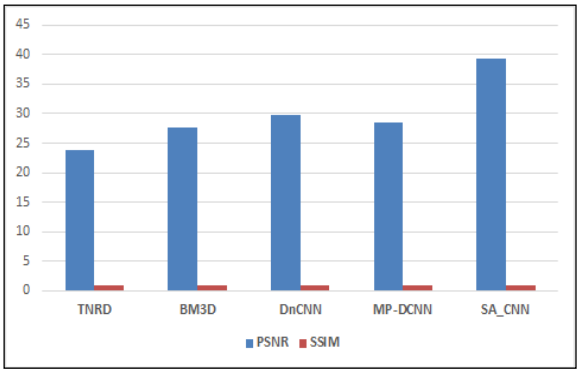

FIGURE 5. Average Peak signal to noise ratio and Structural similarity index of different methods compared with the proposed framework.

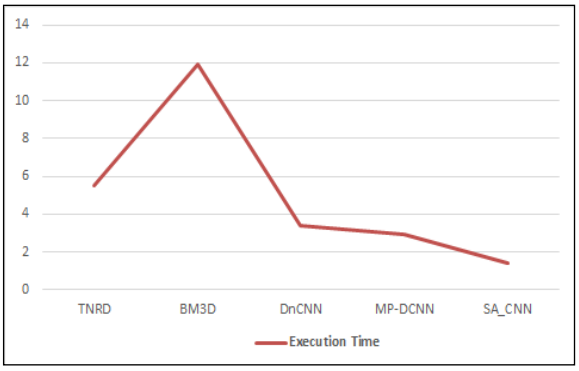

FIGURE 6. Comparative analysis of execution time.

then better the preservation of the inner details of the image. The proposed model has reached up to 0.81 means there is a lot of similarity between original and resultant images.

The average PSNR and SSIM along with efficiency (computational time) of the proposed framework are demonstrated in figures 5 and 6 respectively. It illustrates that the proposed framework achieved improved outcomes than

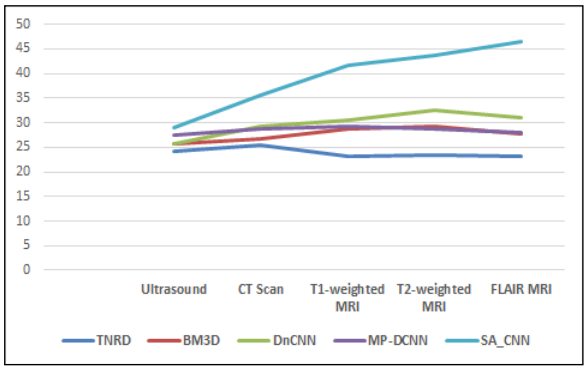

FIGURE 7. Peak signal to noise ratio of different methods compared with the proposed framework.

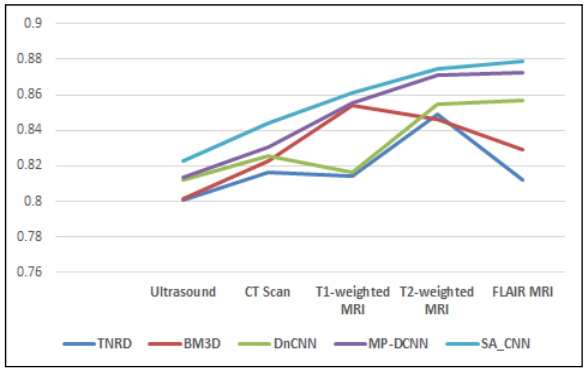

FIGURE 8. Structural similarity index of different methods compared with the proposed framework.

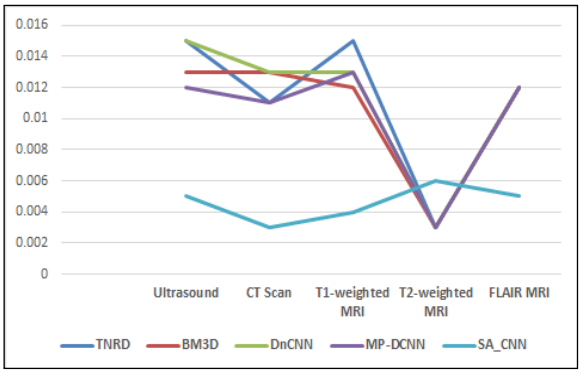

FIGURE 9. Mean squared error of different methods compared with the proposed framework.

other methods. The average PSNR and SSIM are higher than other methods show that the proposed method is best among all. The visualized representation of the performance measures like PSNR and SSIM are done in figures 7 and 8. The proposed framework provides the best outcome as compared to other denoising approaches. The efficiency in terms of seconds for all techniques is shown in figure 6. It can be demonstrated that the proposed SA_CNN eliminates the noise and improves the visual quality details of an image with preserving the edges within an image.

Figure 9, illustrates the MSE value of the proposed framework. The different modalities used in the

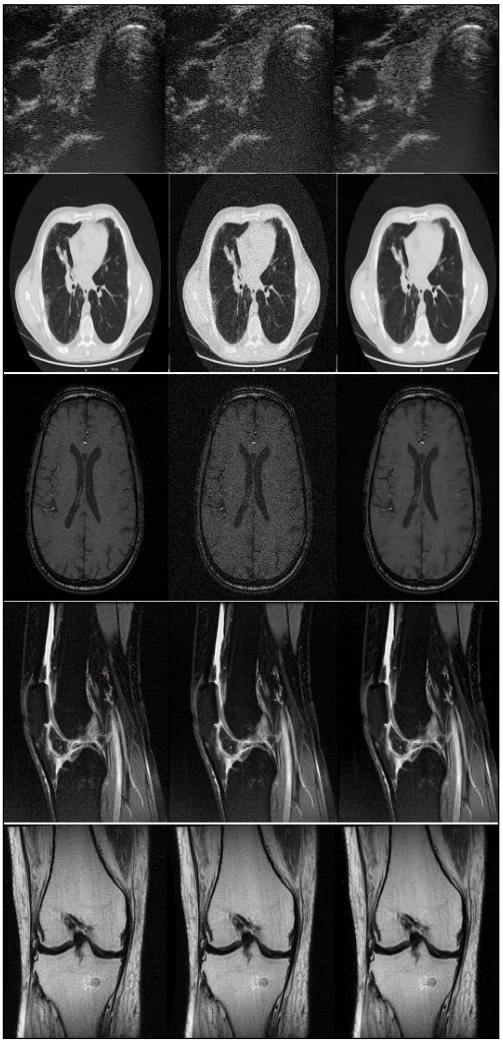

FIGURE 10. First column: Images with noise, Second column: Input image, Third Column: Enhanced and denoised image, First Row: Ultrasound Image, Second Row: CT Scan, Third Row: T1-weighted MRI, Fourth Row: T2-weighted MRI, Fifth Row: Flair MRI.

experimentation along with denoised images are shown in figure 10. The first column has a lot of noise-induced in the image which provides corrupted and irregular visual quality and blurriness in the image. The second column is the input image that is used for experimentation. The third column illustrates the denoised and enhanced best quality image which can be used for further processing. The outcome of the proposed model is denoised using a sparse aware convolution neural network that provides the best precision. Each row in figure 10, displays a different type of image used to validate the real data and performance of the model.

VI. CONCLUSION

A novel sparse aware convolution neural network (SA_CNN) model was proposed in the research. Irregular quality and noise are the main issues in the medical images which leads to inefficient and inaccurate classification outcomes. In the research, the patch creation technique divides the image into various regions and by preparing the dictionary which was utilized for training and testing phases with a convolution neural network. The algorithm was validated by experts (observers) in the respective field of study and cross-validated on different medical datasets. These denoised and high-quality images are stored in the IoHT cloud for ease of access for stakeholders. The security and privacy issues are resolved with the use of vault and challenging schemes. The sessions between IoT devices and servers provided more security from attacks with key changing policy. The proposed technique (SA_CNN) was compared with different methods like TNRD, BM3D, DnCNN, and MP-DCNN, been measured as PSNR, SSIM, and MSE parameters. In the research, the proposed model was used on diverse kinds of images like Ultrasound, CT scan, T1-weighted MRI, T2-weighted MRI, and Flair MRI. The proposed model achieved better denoised and increased visual quality images with extensive experimental outcomes. The proposed SA_CNN technique achieved more than 40dB of PSNR and 0.85 SSIM values for MR images. The experimental outcomes show the proposed method is very competitive with other state-of-the-art methods for denoising.

This research work describes a variety of approaches along with the Internet of Healthcare Things (IoHT) and comparative analysis with SAR investigation with different medical modalities, which is the future scope of further investigation. The proposed work limits in terms of SSIM value 0.8509 for modality such as T1-weighted images. In the future, we utilize CNN with prior knowledge to deal with complex blurred and color images. Further, the cloud IoT concept can be used for providing security with more protocols for the session and key management.

ACKNOWLEDGMENT

The authors would like to thank Dr. R. S. Muchchandi, Director and Chief Radiologist, Vagus Super Specialist Hospital, Bengaluru, India, for providing the medical image datasets.

REFERENCES

[1] U. Ghosh, P. Chatterjee, S. Shetty, and R. Datta, "An SDN-IoT-based framework for future smart cities: Addressing perspective," in *Internet of Things and Secure Smart Environments: Successes and Pitfalls*. Boca Raton, FL, USA: CRC Press, 2020.

[2] W. Alnumay, U. Ghosh, and P. Chatterjee, "A trust-based predictive model for mobile ad hoc network in Internet of Things," *Sensors*, vol. 19, no. 6, p. 1467, Mar. 2019, doi: 10.3390/s19061467.

[3] A. Maity, A. Pattanaik, S. Sagnika, and S. Pani, "A comparative study on approaches to speckle noise reduction in images," in *Proc. Int. Conf. Comput. Intell. Netw.*, Bhubaneswar, India, Jan. 2015, pp. 148–155, doi: 10.1109/CINE.2015.36.

[4] A. Phophalia and S. K. Mitra, "Rough set based bilateral filter design for denoising brain MR images," *Appl. Soft Comput.*, vol. 33, pp. 1–14, Aug. 2015, doi: 10.1016/j.asoc.2015.04.005.

[5] C. Huerga, L. Glaría, P. Castro, L. Alejo, J. Bayón, and E. Guibelalde, "Segmentation improvement through denoising of PET images with 3D-context modelling in wavelet domain," *Phys. Medica*, vol. 53, pp. 62–71, Sep. 2018, doi: 10.1016/j.ejmp.2018.08.008.

[6] C. Rubini and N. Pavithra, "Contrast enhancement of MRI images using AHE and CLAHE techniques," *Int. J. Innov. Technol. Exploring Eng.*, vol. 9, no. 2, pp. 2442–2445, Dec. 2019, doi: 10.35940/ijitee.B7017.129219.

[7] Ravichandran, "An efficient method for contrast enhancement in still images using histogram modification framework," *J. Comput. Sci.*, vol. 8, no. 5, pp. 775–779, May 2012, doi: 10.3844/jcssp.2012.775.779.

[8] N. Salem, H. Malik, and A. Shams, "Medical image enhancement based on histogram algorithms," *Procedia Comput. Sci.*, vol. 163, pp. 300–311, Jan. 2019, doi: 10.1016/j.procs.2019.12.112.

[9] J. Chen, W. Yu, J. Tian, L. Chen, and Z. Zhou, "Image contrast enhancement using an artificial bee colony algorithm," *Swarm Evol. Comput.*, vol. 38, pp. 287–294, Feb. 2018, doi: 10.1016/j.swevo.2017.09.002.

[10] A. B. Huddin, W. M. D. W Zaki, A. C. Wai Mun, L. C. Siong, and H. A. Hamid, "Enhancement techniques for MRI human spine images," *Jurnal Teknologi*, vol. 77, no. 6, pp. 1–7, Nov. 2015, doi: 10.11113/jt.v77.6221.

[11] I. S. Isa, S. N. Sulaiman, M. Mustapha, and N. K. A. Karim, "Automatic contrast enhancement of brain MR images using average intensity replacement based on adaptive histogram equalization (AIR-AHE)," *Biocybernetics Biomed. Eng.*, vol. 37, no. 1, pp. 24–34, 2017, doi: 10.1016/j.bbe.2016.12.003.

[12] P. Kandhway, A. K. Bhandari, and A. Singh, "A novel reformed histogram equalization based medical image contrast enhancement using krill herd optimization," *Biomed. Signal Process. Control*, vol. 56, Feb. 2020, Art. no. 101677, doi: 10.1016/j.bspc.2019.101677.

[13] K. Chen, X. Lin, X. Hu, J. Wang, H. Zhong, and L. Jiang, "An enhanced adaptive non-local means algorithm for Rician noise reduction in magnetic resonance brain images," *BMC Med. Imag.*, vol. 20, Jan. 2020, Art. no. 2, doi: 10.1186/s12880-019-0407-4.

[14] M. N. Ali, "A wavelet-based method for MRI liver image denoising," *Biomed. Eng./Biomedizinische Technik*, vol. 64, no. 6, pp. 699–709, Dec. 2019, doi: 10.1515/bmt-2018-0033.

[15] X. You, N. Cao, H. Lu, M. Mao, and W. Wanga, "Denoising of MR images with Rician noise using a wider neural network and noise range division," *Magn. Reson. Imag.*, vol. 64, pp. 154–159, Dec. 2019, doi: 10.1016/j.mri.2019.05.042.

[16] J. Yuan, "MRI denoising via sparse tensors with reweighted regularization," *Appl. Math. Model.*, vol. 69, pp. 552–562, May 2019, doi: 10.1016/j.apm.2019.01.011.

[17] F. Baselice, G. Ferraioli, V. Pascazio, and A. Sorriso, "Denoising of MR images using Kolmogorov-Smirnov distance in a non local framework," *Magn. Reson. Imag.*, vol. 57, pp. 176–193, Apr. 2019, doi: 10.1016/j.mri.2018.11.022.

[18] H. V. Bhujle and B. H. Vadavadagi, "NLM based magnetic resonance image denoising—A review," *Biomed. Signal Process. Control*, vol. 47, pp. 252–261, Jan. 2019, doi: 10.1016/j.bspc.2018.08.031.

[19] M. Elhoseny and K. Shankar, "Optimal bilateral filter and convolutional neural network based denoising method of medical image measurements," *Measurement*, vol. 143, pp. 125–135, Sep. 2019, doi: 10.1016/j.measurement.2019.04.072.

[20] M. Judson, T. Viger, and H. Lim, "Efficient and robust non-local means denoising methods for biomedical images," in *Proc. ITM Web Conf.*, vol. 29, 2019, Art. no. 01003, doi: 10.1051/itmconf/20192901003.

[21] J. Mohan, V. Krishnaveni, and Y. Guo, "Performance comparison of MRI denoising techniques based on neutrosophic set approach," *Eur. J. Sci. Res.*, vol. 86 no. 3, pp. 307–318, 2012.

[22] H. M. Rai and K. Chatterjee, "Hybrid adaptive algorithm based on wavelet transform and independent component analysis for denoising of MRI images," *Measurement*, vol. 144, pp. 72–82, Oct. 2019, doi: 10.1016/j.measurement.2019.05.028.

[23] M. Sahnoun, F. Kallel, M. Dammak, O. Kammoun, C. Mhiri, K. B. Mahfoudh, and A. B. Hamida, "A modified DWT-SVD algorithm for T1-w brain MR images contrast enhancement," *IRBM*, vol. 40, no. 4, pp. 235–243, Aug. 2019, doi: 10.1016/j.irbm.2019.04.007.

[24] N. Otsu, "A threshold selection method from gray-level histograms," *IEEE Trans. Syst., Man, Cybern.*, vol. SMC-9, no. 1, pp. 62–66, Jan. 1979, doi: 10.1109/TSMC.1979.4310076.

[25] J. Sijbers, A. J. den Dekker, J. Van Audekerke, M. Verhoye, and D. Van Dyck, "Estimation of the noise in magnitude MR images," *Magn. Reson. Imag.*, vol. 16, no. 1, pp. 87–90, 1998, doi: 10.1016/S0730-725X(97)00199-9.

[26] J. Sijbers, A. J. den Dekker, P. Scheunders, and D. Van Dyck, "Maximum-likelihood estimation of rician distribution parameters," *IEEE Trans. Med. Imag.*, vol. 17, no. 3, pp. 357–361, Jun. 1998, doi: 10.1109/42.712125.

[27] J. Sijbers and A. J. den Dekker, "Maximum likelihood estimation of signal amplitude and noise variance from MR data," *Magn. Reson. Med.*, vol. 51, pp. 586–594, Mar. 2004, doi: 10.1002/mrm.10728.

[28] Sujeet More, MRI Dataset, Bengaluru, India. *Vagus Super Speciality Hospital*. [Online]. Available: https://drive.google.com/drive/folders/1Opanl81KJ7Z5E4S91incA9FpfY3fbdGn?usp=sharing

[29] C. Singh, S. K. Ranade, and K. Singh, "Invariant moments and transform-based unbiased nonlocal means for denoising of MR images," *Biomed. Signal Process. Control*, vol. 30, pp. 13–24, Sep. 2016, doi: 10.1016/j.bspc.2016.05.007.

[30] I. S. Isa, S. N. Sulaiman, M. Mustapha, and S. Darus, "Evaluating denoising performances of fundamental filters for T2-weighted MRI images," *Procedia Comput. Sci.*, vol. 60, pp. 760–768, 2015, doi: 10.1016/j.procs.2015.08.231.

[31] S. Lahmiri and M. Boukadoum, "Biomedical image denoising using variational mode decomposition," in *Proc. IEEE Biomed. Circuits Syst. Conf. (BioCAS)*, Oct. 2014, pp. 340–343, doi: 10.1109/BioCAS.2014.6981732.

[32] S. Lahmiri, "Image denoising in bidimensional empirical mode decomposition domain: The role of Student's probability distribution function," *Healthcare Technol. Lett.*, vol. 3, no. 1, pp. 67–71, Mar. 2016, doi: 10.1049/htl.2015.0007.

[33] Y. Sun, F. P.-W. Lo, and B. Lo, "Security and privacy for the Internet of medical things enabled healthcare systems: A survey," *IEEE Access*, vol. 7, pp. 183339–183355, 2019, doi: 10.1109/ACCESS.2019.2960617.

[34] A. Aljamel, T. Osman, G. Acampora, A. Vitiello, and Z. Zhang, "Smart information retrieval: Domain knowledge centric optimization approach," *IEEE Access*, vol. 7, pp. 4167–4183, 2019, doi: 10.1109/ACCESS.2018.2885640.

[35] Q. Cai, H. Wang, Z. Li, and X. Liu, "A survey on multimodal data-driven smart healthcare systems: Approaches and applications," *IEEE Access*, vol. 7, pp. 133583–133599, 2019, doi: 10.1109/ACCESS.2019.2941419.

[36] Y. Chen, Q. Zhao, X. Hu, and B. Hu, "Multi-resolution parallel magnetic resonance image reconstruction in mobile computing-based IoT," *IEEE Access*, vol. 7, pp. 15623–15633, 2019, doi: 10.1109/ACCESS.2019.2894694.

[37] M. Elhoseny, G. Ramirez-Gonzalez, O. M. Abu-Elnasr, S. A. Shawkat, N. Arunkumar, and A. Farouk, "Secure medical data transmission model for IoT-based healthcare systems," *IEEE Access*, vol. 6, pp. 20596–20608, 2018, doi: 10.1109/ACCESS.2018.2817615.

[38] S. Gai and Z. Bao, "New image denoising algorithm via improved deep convolutional neural network with perceptive loss," *Expert Syst. Appl.*, vol. 138, Dec. 2019, Art. no. 112815, doi: 10.1016/j.eswa.2019.07.032.

[39] C. Tian, Y. Xu, and W. Zuo, "Image denoising using deep CNN with batch renormalization," *Neural Netw.*, vol. 121, pp. 461–473, Jan. 2020, doi: 10.1016/j.neunet.2019.08.022.

[40] H. R. Shahdoosti and Z. Rahemi, "Edge-preserving image denoising using a deep convolutional neural network," *Signal Process.*, vol. 159, pp. 20–32, Jun. 2019, doi: 10.1016/j.sigpro.2019.01.017.

[41] K. Dabov, A. Foi, V. Katkovnik, and K. Egiazarian, "Image denoising by sparse 3-D transform-domain collaborative filtering," *IEEE Trans. Image Process.*, vol. 16, no. 8, pp. 2080–2095, Aug. 2007, doi: 10.1109/TIP.2007.901238.

[42] Y. Chen and T. Pock, "Trainable nonlinear reaction diffusion: A flexible framework for fast and effective image restoration," *IEEE Trans. Pattern Anal. Mach. Intell.*, vol. 39, no. 6, pp. 1256–1272, Jun. 2017, doi: 10.1109/TPAMI.2016.2596743.

[43] K. Zhang, W. Zuo, Y. Chen, D. Meng, and L. Zhang, "Beyond a Gaussian denoiser: Residual learning of deep CNN for image denoising," *IEEE Trans. Image Process.*, vol. 26, no. 7, pp. 3142–3155, Jul. 2017, doi: 10.1109/TIP.2017.2662206.

[44] J. J. P. C. Rodrigues, D. B. De Rezende Segundo, H. A. Junqueira, M. H. Sabino, R. M. Prince, J. Al-Muhtadi, and V. H. C. De Albuquerque, "Enabling technologies for the Internet of health things," *IEEE Access*, vol. 6, pp. 13129–13141, 2018, doi: 10.1109/ACCESS.2017.2789329.

SUJEET MORE received the bachelor's degree and the master's degree in computer science and engineering from Visvesvaraya Technological University, Belgaum, in 2011 and 2013, respectively. He is currently pursuing the Ph.D. degree with the School of Computer Science and Engineering, Lovely Professional University, Jalandhar, Punjab. Since 2013, he has been working as an Assistant Professor. He has published many articles in national and international conferences and reputed journals. He is a reviewer of several journals, including the *Journal of Intelligent and Fuzzy Systems* and the *International Journal of Intelligent Information Systems*. His areas of interest are machine learning, cloud computing, and the IoT. He was a Guest Editor of a special issue published by Science Publication Group, USA.

JIMMY SINGLA is an academician and administrator with 8 years of experience in Teaching, Administration, and Research and Development. He is an Associate Professor in School of Computer Science and Engineering at Lovely Professional University, Punjab. He has also worked as HOD (CSE) and Coordinator (Academics) at IKG PTU Campus Hoshiarpur. He has completed Ph.D in Computer Science and Engineering under the supervision of Dr. Dinesh Grover (Alumnus IIT Roorkee), retired Professor cum Head, Department of Computer Science and Electrical Engineering, Punjab Agricultural University, Ludhiana. The area of specialization of Dr. Singla includes Artificial Intelligence, Expert-Systems, etc. Dr. Singla has more than 30 research publications in various national, international conferences and journals to his credit. Presently, he is supervisor of 6 Ph.D and 2 M.Tech scholars. He is reviewer of IEEE conferences, indexed books, and also an editorial board member of many referred journals. He is awarded as "*Gems of Jagraon*" from Zenith welfare society and Book bank Jagraon in 2004. He has also been honored with the "*The Best Teacher*" from the Management of North West Group of Institutions, Moga on the occasion of Teacher's day in 2013. He has taught various subjects like Software Engineering, Software Project Management, Expert System, Computer Networks, Operating System, and Machine Learning.

SAHIL VERMA (Member, IEEE) received the B.Tech. and M.Tech. degrees from Maharishi Markandeshwar University, Mullana, India, in 2012, and the Ph.D. degree from Jaipur National University, Jaipur, India, in 2017, all in computer science and engineering. He is currently working as an Associate Professor with Lovely Professional University, Phagwara, India. He has many research contributions in the area of cloud computing, the Internet of Things, vehicular *ad-hoc* networks, WSN, and MANET. Some of his research findings are published in top-cited journals, such as the IEEE, Wiley. Various international conferences of repute. He is a member of ACM, IAENG, and an editorial board member of many international journals. He has chaired many sessions in reputed international conferences abroad and India. He has guided 14 P.G. students and three Ph.D. students and six are ongoing. He has visited many universities in abroad and India.

KAVITA (Member, IEEE) received the B.Tech. and M.Tech. degree from Maharishi Markandeshwar University, Mullana, India, in 2012, and the Ph.D. degree from Jaipur National University, Jaipur, India, in 2018, all in computer science and engineering. She is currently working as an Associate Professor with Lovely Professional University, Phagwara, India. She has many research contributions in the area of cloud computing, the Internet of Things, vehicular ad-hoc networks, WSN, and MANET. Some of her research findings are published in top-cited journals, such as the IEEE, Wiley. Various international conferences of repute. She is a member of ACM, IAENG, and an editorial board member of many international journals. She has chaired many sessions in reputed international conferences abroad and India. She is guiding six Ph.D. students. She has visited many universities out of these two are international universities (Italy and the Czech Republic).

UTTAM GHOSH (Senior Member, IEEE) received the Ph.D. degree in electronics and electrical engineering from the Indian Institute of Technology Kharagpur, India, in 2013. He was Postdoctoral Experience with the University of Illinois in Urbana-Champaign, Fordham University, and Tennessee State University. He is currently working as an Assistant Professor with the Department of Electrical Engineering and Computer Science, Vanderbilt University, Nashville, TN, USA. He has published 55 papers at reputed international journals, including the IEEE TRANSACTION, Elsevier, Springer, IET, Wiley, Inder-Science, and IETE, and also in top international conferences sponsored by IEEE, ACM, and Springer. He is a member of AAAS, ASEE, ACM, and Sigma Xi. He is actively working for editing two edited volumes on Emerging CPS, Security, and Machine / Machine Learning with CRC Press, and Chapman Hall Big Data Series. His main research interests include cybersecurity, computer networks, wireless networks, information-centric networking, and software-defined networking.

JOEL J. P. C. RODRIGUES (Fellow, IEEE) is currently a Professor with the National Institute of Telecommunications (Inatel), Brazil, a Senior Researcher with the Instituto de Telecomunicações, Portugal, and a Visiting Professor with the Federal University of Piauí, Brazil. He is also the Leader of the Internet of Things research group (CNPq), the Director for Conference Development - IEEE ComSoc Board of Governors, an IEEE Distinguished Lecturer, the Technical Activities Committee Chair of the IEEE ComSoc Latin America Region Board, the President of the scientific council at ParkUrbis–Covilhã Science and Technology Park, the Past-Chair of the IEEE ComSoc Technical Committee on eHealth, the Past-Chair of the IEEE ComSoc Technical Committee on Communications Software, a Steering Committee member of the IEEE Life Sciences Technical Community and a Publications Co-Chair, and a Member Representative of the IEEE Communications Society on the IEEE Biometrics Council. He has authored or coauthored over 850 papers in refereed international journals and conferences, three books, and two patents. He is a member of many international TPCs and participated in several international conferences organization. He is a licensed Professional Engineer (as a Senior Member), a member of the Internet Society, and a Senior Member of ACM. He received several Outstanding Leadership and Outstanding Service Awards by the IEEE Communications Society and several best papers awards. He has been the General Chair and the TPC Chair of many international conferences, including IEEE ICC, IEEE GLOBECOM, IEEE HEALTHCOM, and IEEE LatinCom. He is the Editor-in-Chief of the *International Journal on E-Health and Medical Communications* and an editorial board member of several high-reputed journals.

A. S. M. SANWAR HOSEN received the M.S. and Ph.D. degrees in CSE from Jeonbuk National University, in 2013 and 2017, respectively. He worked as a Postdoctoral Researcher with the School of Computer, Information and Communication Engineering, Kunsan National University, Gunsan, South Korea, and with the Division, Jeonbuk National University (JBNU), Jeonju, South Korea. He is currently an Assistant Professor (Research) with the Division of Computer Science and Engineering (CSE), JBNU. He has published several articles in journals and international conferences and serves as a reviewer of several reputed journals. His research interests are in wireless sensor networks, the Internet of Things, network security, data distribution services, fog-cloud computing, artificial intelligence, blockchain, and green IT.

IN-HO RA (Member, IEEE) received the M.S. and Ph.D. degrees in computer engineering from Chung-Ang University, Seoul, South Korea, in 1991 and 1995, respectively. From 2007 to 2008, he was a Visiting Scholar with the University of South Florida, Tampa. He is currently a Professor with the School of Computer, Information and Communication Engineering, Kunsan National University, Kunsan, South Korea. His research interests include wireless ad-hoc and sensor networks, cross-layer network protocol, cognitive radio, PS-LTE, and the IoT.